

Testing predictions of electron scale ETG pedestal turbulence in DIII-D ELMy H-modes

W. Guttenfelder¹, R.J. Groebner², B. Grierson¹,
J.M. Canik³, E. Belli², J. Candy², A. Ashourvan¹

¹PPPL, ²General Atomics, ³ORNL

MIT PSFC seminar
May 3, 2019

Acknowledgements:

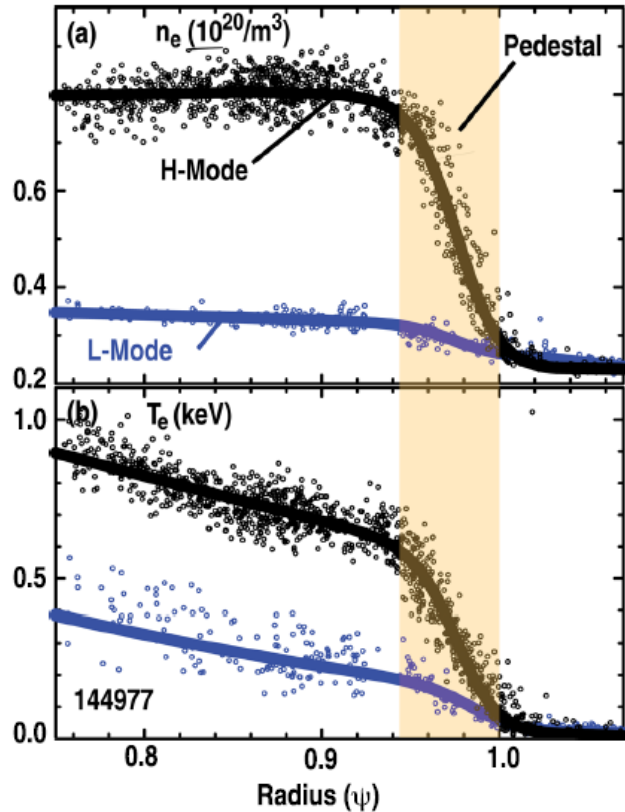
NERSC resources, DOE funding
A. Diallo, F. Laggner, P.B. Snyder
D.R. Hatch, M. Kotschenreuther



Overview / Summary

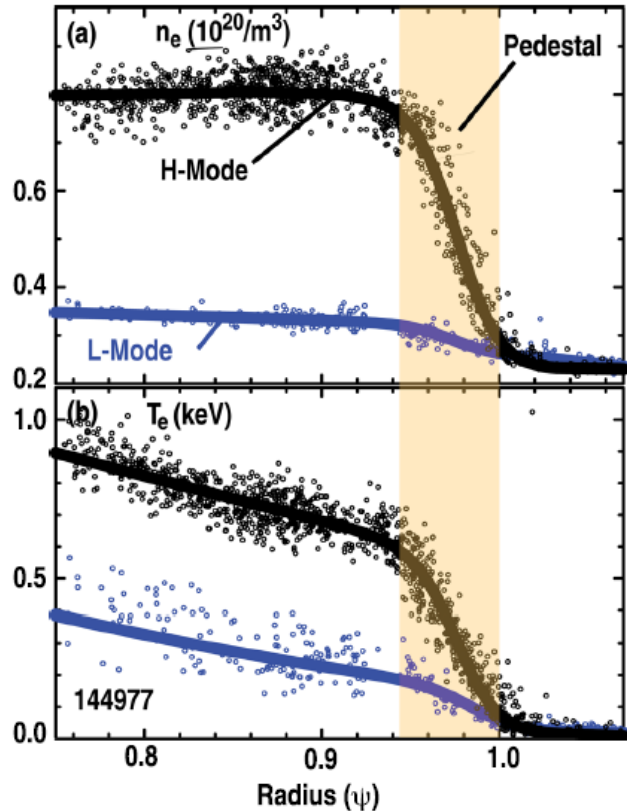
- **Linear gyrokinetic analysis (CGYRO) suggests electron scale ETG turbulent transport may limit $\eta_e \sim \nabla T_e / \nabla n_e$ in some DIII-D ELMy H-mode pedestals**
- **Numerous *nonlinear* gyrokinetic simulations run to predict ETG transport, used to develop ETG pedestal transport model for use in predictive simulations**
 - **ETG contributes to $\chi_{e,ped}$, but unlikely to be the only transport mechanism**
 - **Neoclassical D_e plays non-negligible role in setting density profile**

High confinement H-mode characterized by steep gradients in the edge “pedestal” region



A.W. Leonard (2014)

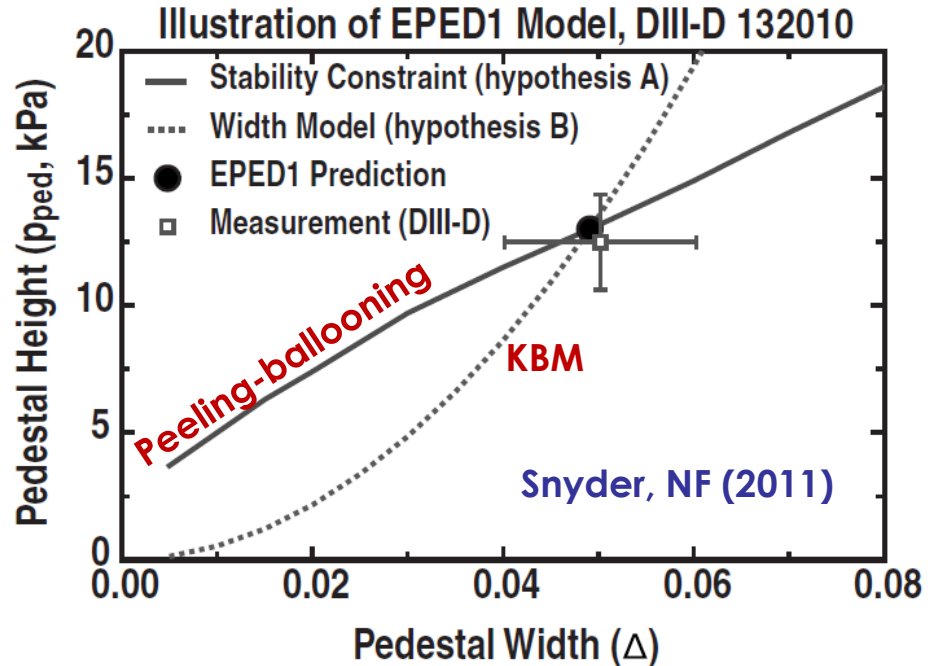
High confinement H-mode characterized by steep gradients in the edge “pedestal” region



A.W. Leonard (2014)

Guttenfelder – ETG pe

- MHD stability [peeling-ballooning stability + KBM ∇p transport limit] provides valuable predictive model for pedestal pressure limit in ELM H-modes



Motivation: Understand what sets pedestal density & temperature structure to develop predictive capability

- **[MHD peeling-ballooning stability] + [KBM ∇p transport limit] provides valuable predictive model for pedestal pressure limit in ELMy H-modes [Snyder, NF 2011]**
 - Requires density as input
 - Can not predict n vs T inter-ELM dynamics (i.e. doesn't "know" about source strengths)
 - KBM predicts $D/\chi \sim 1$, whereas experiment often infers $D/\chi \ll 1$
 - Does not capture ELM-free scenarios or low aspect ratio NSTX scenarios

Motivation: Understand what sets pedestal density & temperature structure to develop predictive capability

- **[MHD peeling-ballooning stability] + [KBM ∇p transport limit] provides valuable predictive model for pedestal pressure limit in ELMy H-modes [Snyder, NF 2011]**
 - Requires a transport model
 - Can not predict pedestal structure
 - KBM pedestal model
 - Does not capture ELM-free scenarios or low aspect ratio NSTX scenarios
- **KBM has a ∇p threshold, expected to be extremely stiff (\sim large $d[Q]/d[\nabla T]$)**
- **There are other instabilities that also have thresholds (typically ∇T and/or ∇n), with varying degrees of stiffness and varying D/χ**

Still need a transport model

An aside: The zoology of microinstabilities (& acronyms)

Ion scales ($k_{\perp}\rho_i \leq \sim 1$)

- (ITG) Ion temperature gradient mode ($\sim \nabla T_i$)
- (TEM) Trapped electron mode ($\sim \nabla T_e, \nabla n_e$)
- (PVG) Parallel velocity gradient mode ($\sim R \nabla \Omega$)
- (MTM) Microtearing modes ($\sim \nabla T_e, \beta_e$)
- (KBM) Kinetic ballooning mode ($\sim \alpha \sim \underline{\nabla P_{\text{tot}}/B_{\theta}^2}$)



Electrostatic modes



Electromagnetic modes

Electron scales ($k_{\perp}\rho_i \gg 1, k_{\perp}\rho_e \sim 1$)

- (ETG) Electron temperature gradient mode ($\sim \nabla T_e$)



Electrostatic mode

• Each *theoretical* instability is distinguished by:

- Scaling with parameters ($a/L_T, a/L_n, \beta, v, \alpha, s, q, \dots$)
- Mode frequency (ion, electron diamagnetic direction)
- Spatial structure (ballooning, tearing; ES, EM)
- Partition of transport ($\Gamma, \Pi, Q \rightarrow D/\chi, \chi_{\phi}/\chi$) ["transport fingerprint", UT-Austin]

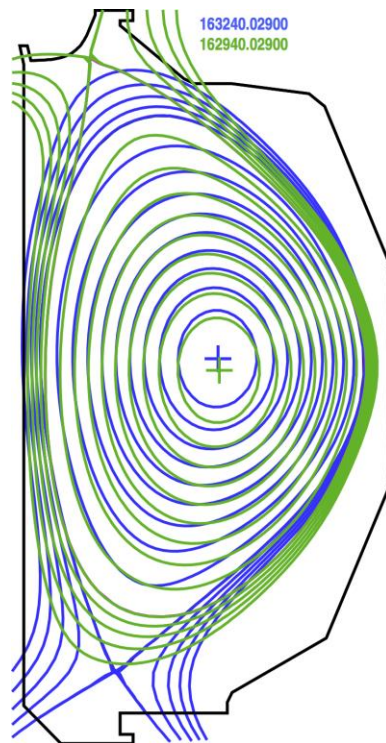
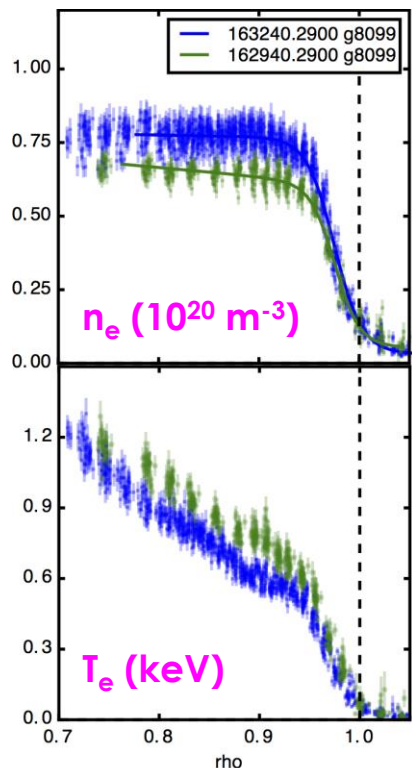
Motivation: Understand what sets pedestal density & temperature structure to develop predictive capability

- [MHD peeling-ballooning stability] + [KBM ∇p transport limit] provides valuable predictive model for pedestal pressure limit in ELMy H-modes [Snyder, NF 2011]
 - Requires pedestal temperature profile
 - Can not predict pedestal temperature profile
 - KBM pedestal model
 - Does not capture ELM-free scenarios or low aspect ratio NSTX scenarios
- **Still need a transport model**
- KBM has a ∇p threshold, expected to be extremely stiff (\sim large $d[Q]/d[\nabla T]$)
- There are other instabilities that also have thresholds (typically ∇T and/or ∇n), with varying degrees of stiffness and varying D/χ
- Hypothesis: A more complete transport model accounting for all instabilities and their thresholds / stiffness, coupled with MHD P-B, could provide a unified understanding for all H-mode/I-mode pedestal structures

Motivation: Understand what sets pedestal density & temperature structure to develop predictive capability

- [MHD peeling-ballooning stability] + [KBM ∇p transport limit] provides valuable predictive model for pedestal pressure limit in ELMy H-modes [Snyder, NF 2011]
 - Requires finite resistivity
 - Can not be used to predict pedestal structure
 - KBM pedestal model is not predictive
 - Does not capture ELM-free scenarios or low aspect ratio NSTX scenarios
- **Still need a transport model**
- KBM has a ∇p threshold, expected to be extremely stiff (\sim large $d[Q]/d[\nabla T]$)
- There are other instabilities that also have thresholds (typically ∇T and/or ∇n), with varying degrees of stiffness and varying D/χ
- Hypothesis: A more complete transport model accounting for all instabilities and their thresholds / stiffness, coupled with MHD P-B, could provide a unified understanding for all H-mode/I-mode pedestal structures
- This talk: Use gyrokinetics (CGYRO) to predict theoretical microinstabilities and transport in DIII-D ELMy H-mode; compare with experimental interpretation using SOLPS-ITER \rightarrow Begin developing ETG pedestal transport model as one component of a predictive model

Investigating pedestal transport in two similar discharges with different edge particle source (baffling / cryopumping)



$I_p = 1.4 \text{ MA}$
 $B_T = (\pm) 2.1 \text{ T}$
 $P_{\text{NBI}} = 3 \text{ MW}$
 $\beta_N = 2$
 $q_{95} = 3.7\text{-}4$

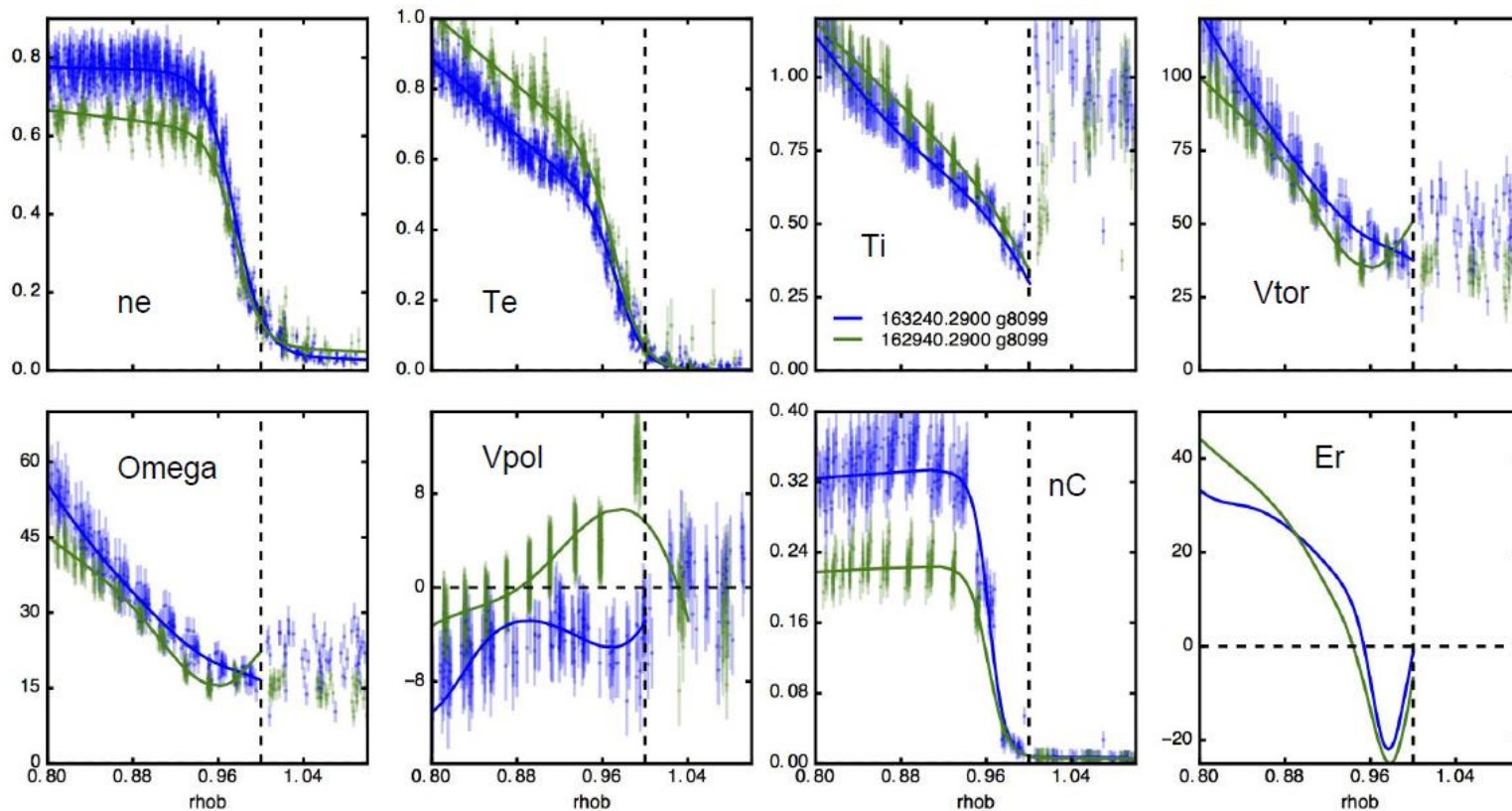
LSN – strike point on lower shelf (\rightarrow open divertor)
USN – strike point in front of cryo baffle (\rightarrow closed divertor)

Flipped B_T to maintain consistent ∇B divertor drifts

Very low/no gas fueling beyond recycling

- USN closed divertor configuration leads to lower $n_{e,\text{ped}}$ due to lower source, higher $T_{e,\text{ped}}$ (Leonard IAEA 2016) \rightarrow what role does transport play?

Kinetic EFIT generated using high resolution edge profiles (ensemble from 80-99% of ELM cycle)



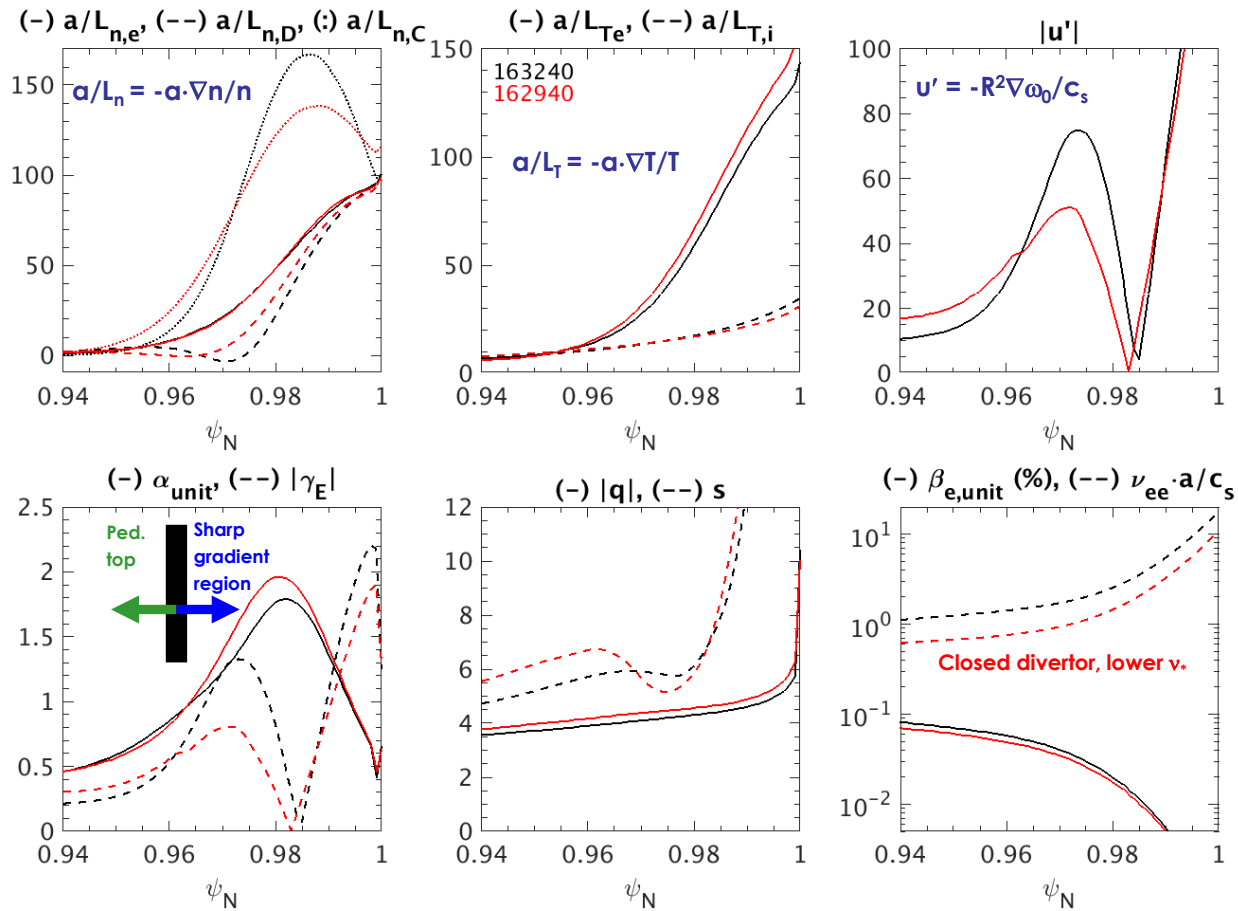
E_r calculated using measured $V_{tor,C}$, $V_{pol,C}$ & ∇P_C

Using spectral, multiscale CGYRO code [Candy, JCP 2016] for scoping linear ion & electron scale instabilities

MODEL CHOICES

- **Uses rigorously derived low- ρ_* drift ordering of Sugama (1998, ...)**
- **Numerical equilibrium using kEFIT (513×513) + 24 harmonic Fourier representation of flux surfaces [Candy, 2009]**
- **3 kinetic species (D,C,e)**
- **Sugama GK collision operator for all species [Candy, 2016; Belli, 2017]**
 - Pseudo-spectral in velocity space (v, ξ)
 - Well-suited for pedestal $v_e \cdot a / c_s \geq 1$
- **Fully electromagnetic ($\phi, \mathbf{A}_{||}, \mathbf{B}_{||}$)**
 - EM effects important at high $\alpha / \alpha_{\text{KBM}}$ in pedestal [Snyder, 2000; ...]
- **Including finite \mathbf{u} & \mathbf{u}' (mach & γ_P ; $\gamma_E=0$) in the low flow limit $\sim O(M)$**
 - Have also tested sonic $O(M^2)$ flow effects [Belli, 2018], possibly important for particle flux [Angioni; Buchholz, 2015]
- **Have tested numerical resolution requirements at each radius**
 - Large parallel resolution (n_θ) required for large gradients ($R/L_{T,n} \gg 1$)

Very strong normalized gradients (n, T and Ω) with large variation across pedestal



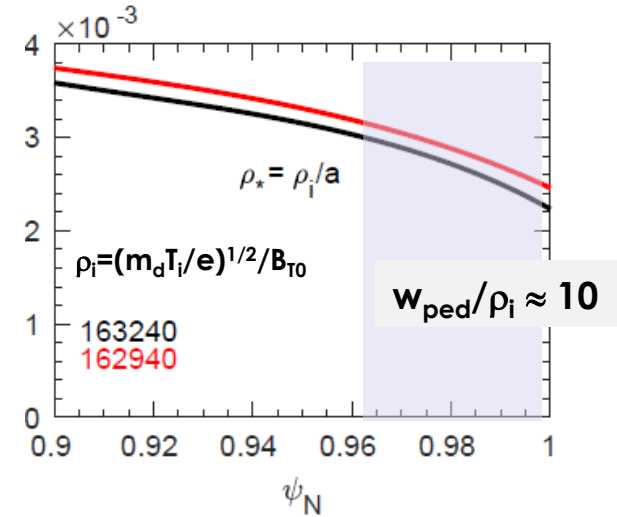
Validity of ion scale simulations in low- ρ_* ordering is questionable across steep gradient region

Across pedestal $\psi_N > 0.96$

$$\rho_{*i} = \rho_i/a \leq 1/300$$

$$\rho_i/\Delta_{\text{ped}} \approx 1/10$$

$L_{c,r}/\Delta_{\text{ped}} \sim 0.5$ [assuming typical turbulence correlation length $L_{c,r} \sim 5 \rho_i$]



- **Profile shearing ($\sim n''$, T'') may be important for ion-scales**
 - Can be tested spectrally in CGYRO, consistent within the framework of low- $\rho_* = \rho/L$ ordering
- **Thermal ion banana widths are comparable to pedestal width, orbit losses not captured**

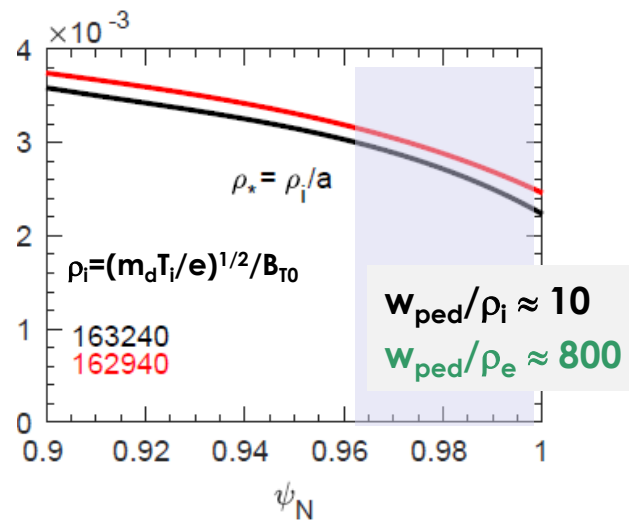
Validity of ion scale simulations in low- ρ_* ordering is questionable across steep gradient region

Across pedestal $\psi_N > 0.96$

$$\rho_{*i} = \rho_i / a \leq 1/300$$

$$\rho_i / \Delta_{\text{ped}} \approx 1/10$$

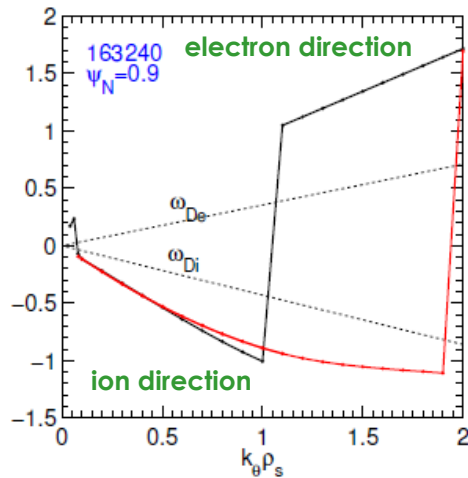
$$L_{c,r} / \Delta_{\text{ped}} \sim 0.5 \text{ [assuming typical turbulence correlation length } L_{c,r} \sim 5 \rho_i \text{]}$$



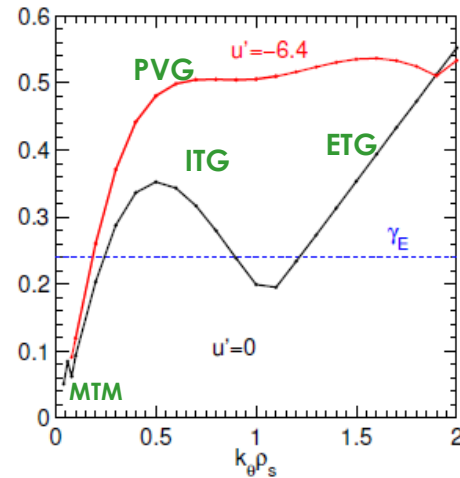
- **Profile shearing ($\sim n''$, T'') may be important for ion-scales**
 - Can be tested spectrally in CGYRO, consistent within the framework of low- $\rho_* = \rho/L$ ordering
 - **Thermal ion banana widths are comparable to pedestal width, orbit losses not captured**
- **Local, δf analysis sufficient for electron scale micro-stability / turbulence analysis ($\rho_e / a \leq 1/6000$)**

Inside pedestal top region ($\psi_N=0.90-0.97$), strong rotation shear leads to broad spectrum of ITG-PVG instabilities with $\gamma_{ion} > \gamma_E$

Real frequencies $\omega_r (c/a)$



$\gamma (c/a)$ Linear growth rates



- Traditional spectra of ITG-ETG found *when not including rotation shear*
- Large rotation shear ($u' = -R^2 \nabla \Omega / c_s = R/a \cdot \gamma_p$) significantly enhances growth rates

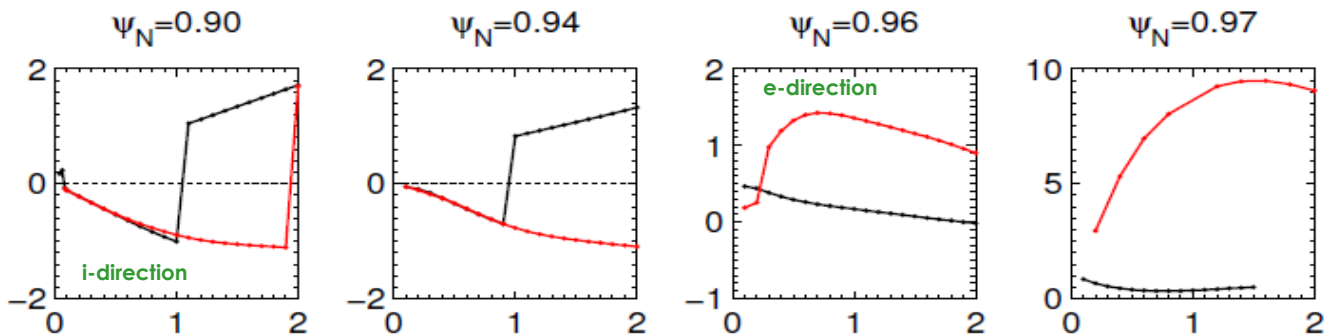
$$R \nabla F_M \rightarrow [R/L_n + R/L_T \cdot (v^2/v_T^2 - 3/2) + (RB_T/R_0 B) \cdot (v_{||}/v_T) \cdot u'] \cdot F_M$$

- Leads to distinct Kelvin-Helmholtz / parallel velocity gradient (PVG) instability [D'Angelo, 1965, Catto et al., 1973, ...]

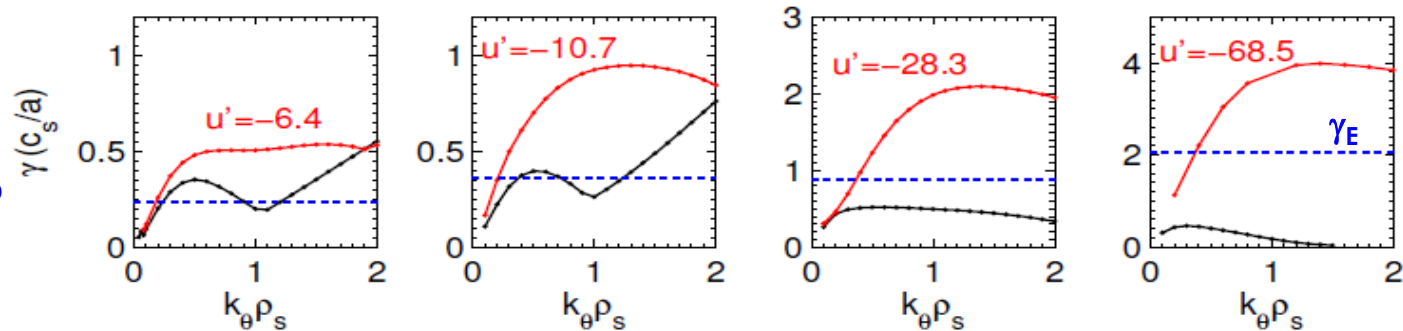
Very similar result moving to pedestal top ($\psi_N=0.96-0.97$);

- Pedestal top: strong drive from u' with $\gamma_{ion} > \gamma_E$; modes transition from i-dia to e-dia ($a/L_{Te} > a/L_{Ti}$)

Real frequencies



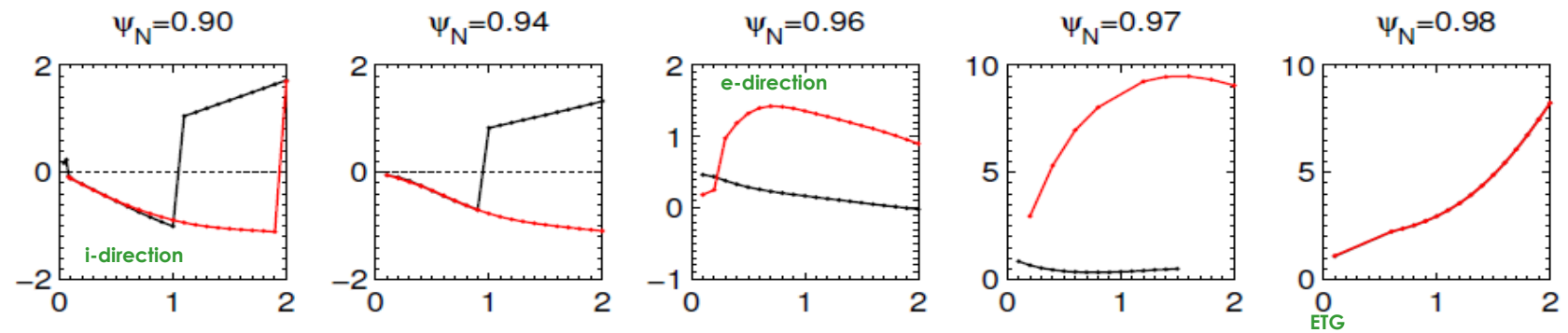
Linear growth rates



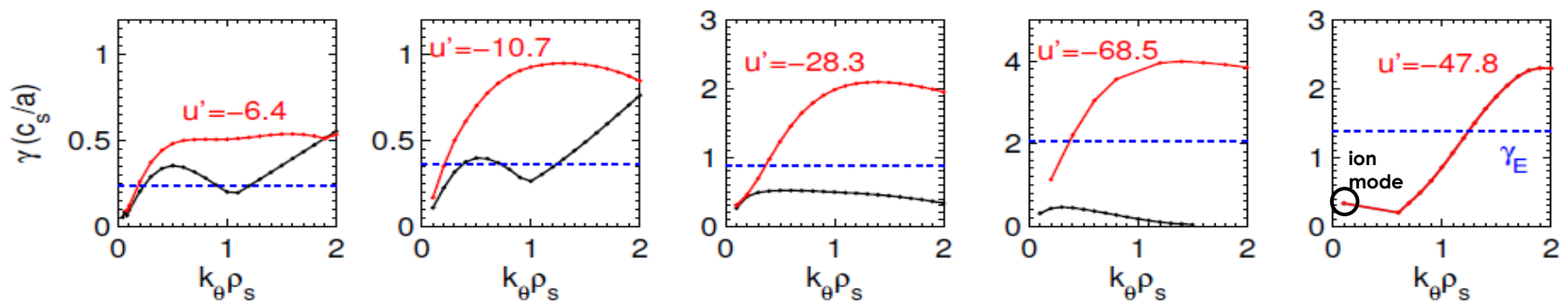
Very similar result moving to pedestal top ($\psi_N=0.96-0.97$); $E \times B$ shearing rate $> \gamma_{lin,ion}$ in sharp gradient region ($\psi_N=0.98$)

- Pedestal top: strong drive from u' with $\gamma_{ion} > \gamma_E$; modes transition from i-dia to e-dia ($a/L_{Te} > a/L_{Ti}$)
- Sharp gradient region ($\psi_N \sim 0.98$): weak ion modes ($\gamma_{lin} < \gamma_E$), no enhancement from u' where $R/L_n > u'$; electromagnetic effects stabilizing; sign of low k_y ETG

Real frequencies

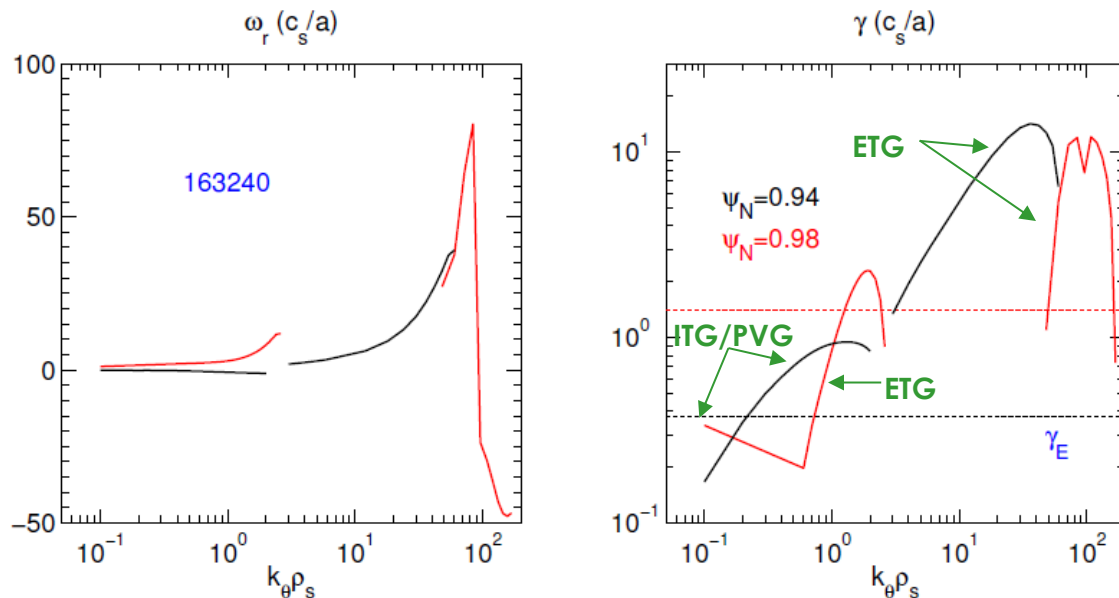


Linear growth rates



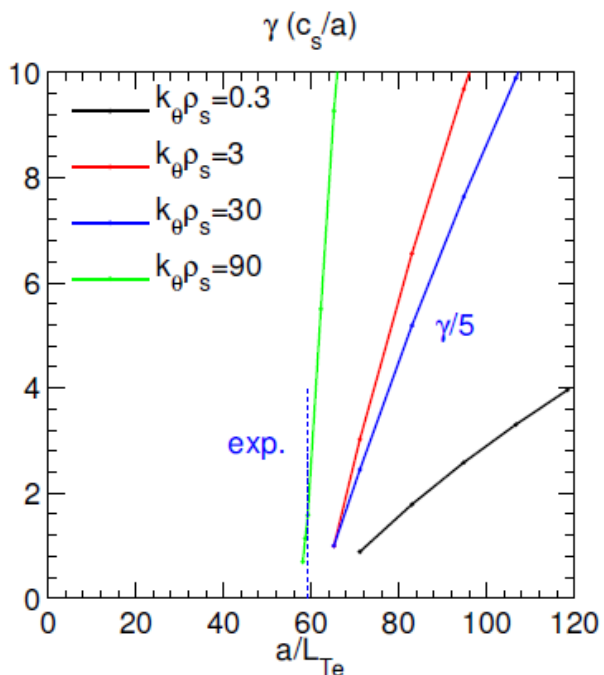
In the sharp gradient region ($\psi_N \sim 0.98$): weak ion modes ($\gamma_{lin} < \gamma_E$), very broad spectrum of ETG

- ETG extends to both $k_\theta \rho_s < 1$ and $k_\theta \rho_s > 100$ for larger a/L_{Te} gradients ($\psi_N = 0.98$)
 - Predicted in AUG [Told, 2008; Hatch, 2015] and NSTX [Canik, 2013; Coury 2016]
- Large low- k_θ / high- k_θ gap at $\psi_N = 0.98$ eliminated w/ marginal ∇T_e increase ($1.2 \times a/L_{Te}$)

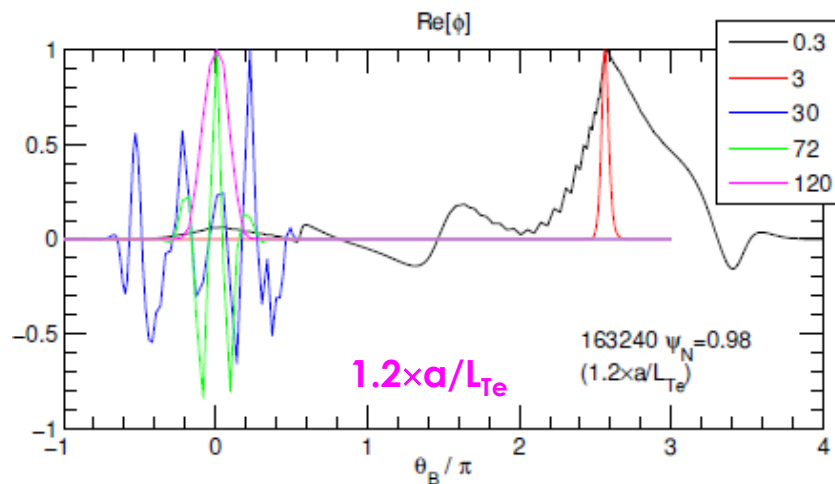


∇T_e near ETG threshold in the sharp gradient region ($\psi_N=0.98$)

- a/L_{Te} sitting near ETG threshold for broad range of wavenumbers $k_{\theta}\rho_s=0.3-90$ ($n\approx 90-26,000$)



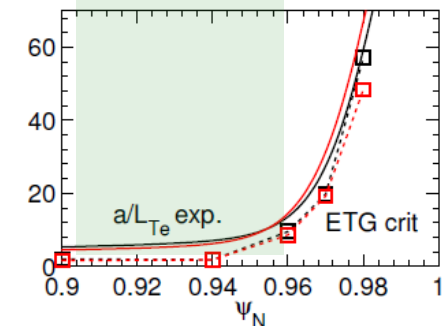
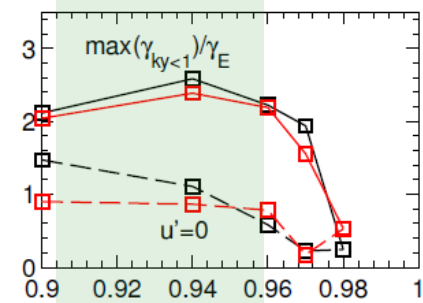
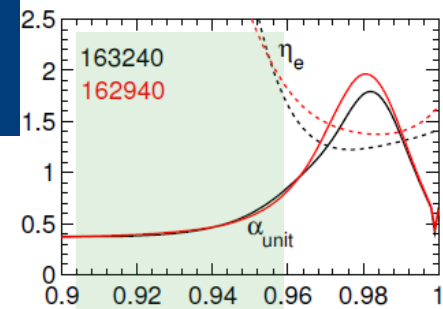
- Large gradient drive excites fine parallel structure, high-order eigenfunction states (e.g. [H. Chen, L. Chen, 2018])
- Lower $k_{\theta}\rho_s$ modes peaking around X-points ($N_{int} * 2\pi \pm 0.6\pi$)
- Highest $k_{\theta}\rho_s \sim 120$ follows more traditional ballooning shape



Linear summary

- Pedestal top ($\psi_N=0.9-0.97$)

- ITG/TEM/PVG modes with growth rates larger than E×B shearing rate ($\gamma_{\text{lin,ion}} > \gamma_E$) → expected to dominate transport



Linear summary

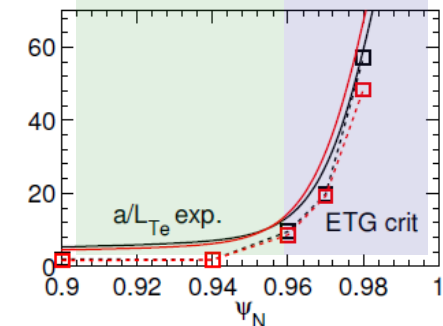
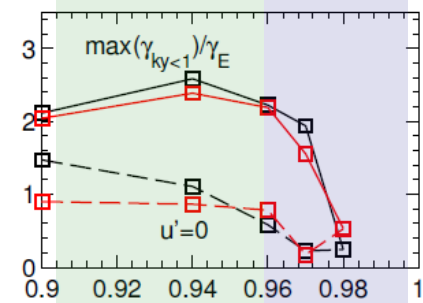
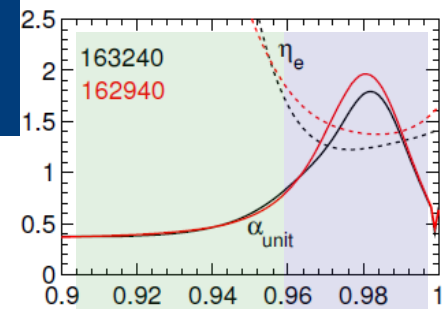
- **Pedestal top ($\psi_N=0.9-0.97$)**

- ITG/TEM/PVG modes with growth rates larger than E×B shearing rate ($\gamma_{lin,ion} > \gamma_E$) → expected to dominate transport

- **Sharp gradient region ($\psi_N = 0.96-0.98$)**

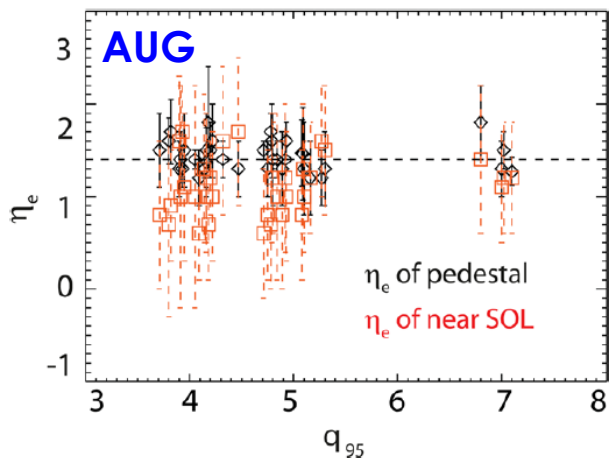
- Ion modes become weak, expect to be suppressed by E×B shearing ($\gamma_E > \gamma_{lin,ion}$) + non-local profile-shearing ($\rho_i/L_T \sim 0.5$)
- ∇T_e follows ETG threshold, $\eta_e = (a/L_{Te}) / (a/L_{ne}) \sim 1.2-1.5$
- Expected for larger R/L_n (e.g. Jenko, 2001, 2009):

$$\left(\frac{R}{L_{Te}}\right)_{ETG}^{crit} = \text{Max} \left[\frac{(1 + Z_{eff} T_e/T_i)(1.3 + 1.9 s/q)(\dots)}{C \cdot R/L_n} \right]$$



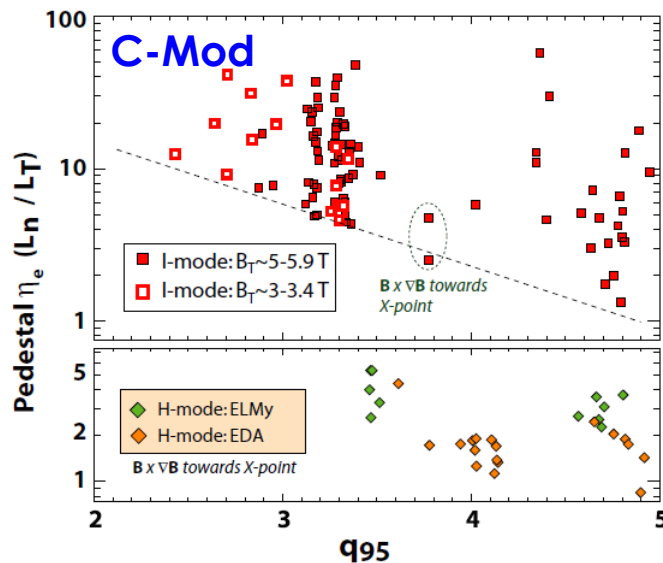
Some experimental evidence for the relevance (or not) of η_e in contributing to pedestal structure

- $\eta_e \sim 1.5-2$ (ELMy H-mode)



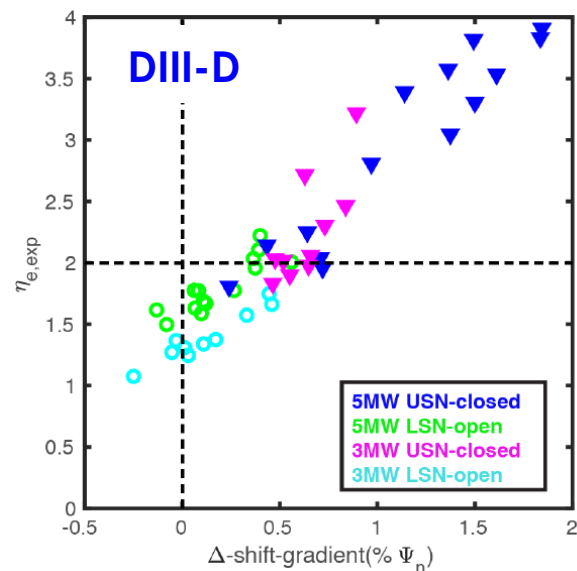
H.J. Sun (2015),
J. Neuhauser (2002)

- $\eta_e \sim 1-2$ (EDA H-mode)
- $\eta_e \sim 2-4$ (ELMy H-mode)
- Even larger for I-mode



D.G. Whyte (2010),
J.W. Hughes (2002)

- η_e varying with divertor closure / fueling / detachment (ELMy H-mode)



H.Q. Wang (2018)

Linear summary

- **Pedestal top ($\psi_N=0.9-0.97$)**

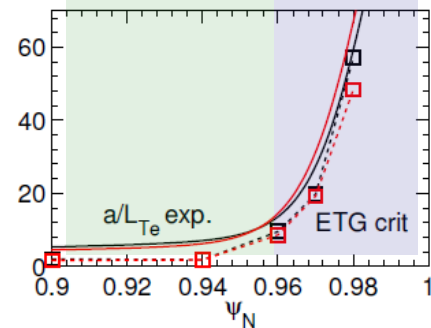
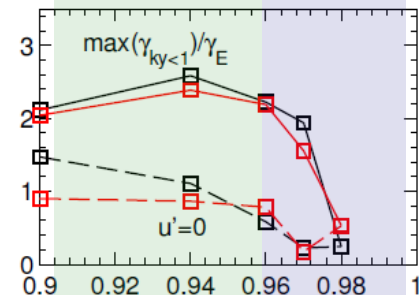
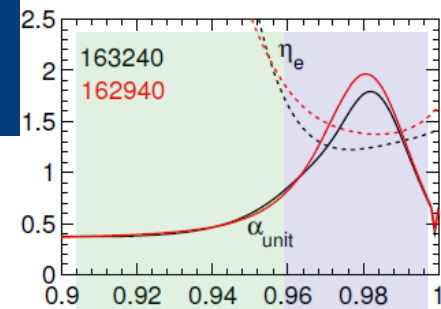
- ITG/TEM/PVG modes with growth rates larger than ExB shearing rate ($\gamma_{lin,ion} > \gamma_E$) \rightarrow expected to dominate transport

- **Sharp gradient region ($\psi_N = 0.96-0.98$)**

- Ion modes become weak, expect to be suppressed by ExB shearing ($\gamma_E > \gamma_{lin,ion}$) + non-local profile-shearing ($\rho_i/L_T \sim 0.5$)
- ∇T_e follows ETG threshold, $\eta_e = (a/L_{Te}) / (a/L_{ne}) \sim 1.2-1.5$
- Expected for larger R/L_n (e.g. Jenko, 2001):

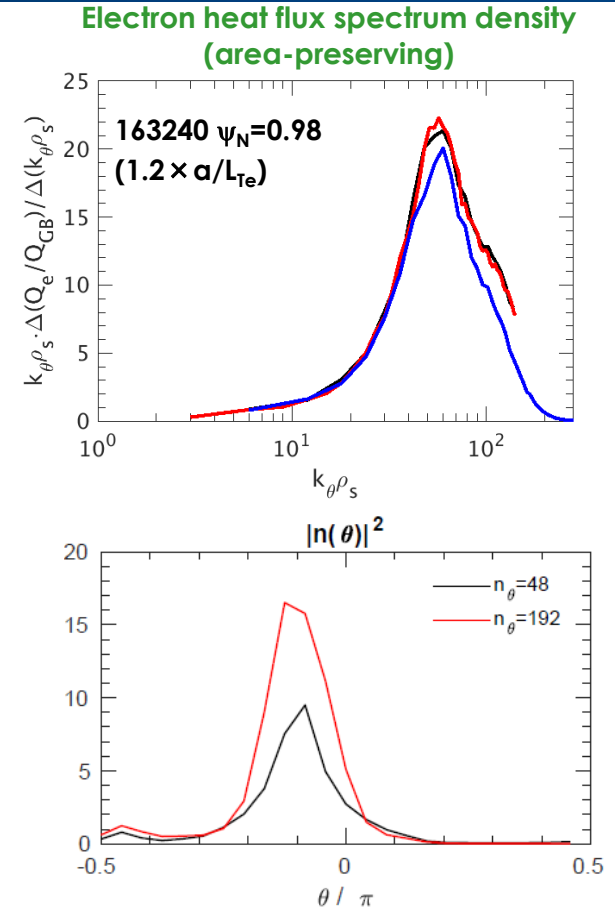
$$\left(\frac{R}{L_{Te}}\right)_{ETG}^{crit} = \text{Max} \left[\frac{(1 + Z_{eff} T_e/T_i)(1.3 + 1.9 s/q)(\dots)}{C \cdot R/L_n} \right]$$

- **Can ETG transport alone account for pedestal structure and changes as source changes? \rightarrow Lets test single-scale nonlinear ETG theory where drift-ordered GK is valid**



Nonlinear ETG simulations saturate with spectral peak at $k_{\theta}\rho_s \sim 50$; turbulence peaks near outboard mid-plane (not X-point)

- **Peak at $k_{\theta}\rho_s \sim 50$ much larger than typical core ETG simulations ($k_{\theta}\rho_{s,peak} \sim 10-15$)**
 - Converged with perpendicular grid parameters
- **Fluctuations peak near outboard mid-plane (not X-point)**
→ $(k_{\theta}\rho_s)_{peak,\theta=0} \sim 10$ (similar to core)
 - $(k_{\theta})_{\theta=0} / k_{\theta} = [(dv/d\theta) / \kappa] = 0.2$ for field-aligned ($\alpha = \varphi - q\psi$) flux coordinates
- **Features similar to those predicted in pedestal of AUG [Hatch, NF 2015] and NSTX [Canik, TTF 2016]**



Nonlinear ETG simulations predict $Q_e \sim 0.2-1.0$ MW using 20% scaled gradients

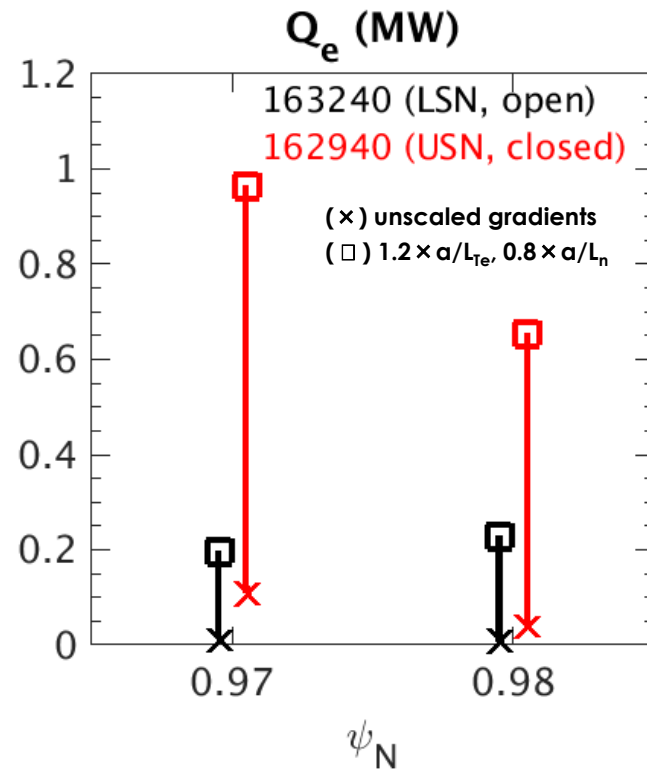
$Q_{e,ETG} < 0.1$ MW (base gradients)

$Q_{e,ETG} = 0.2-1$ MW (20% scaling in ∇n & ∇T)

$Q_{i,NEO} = 0.7$ MW

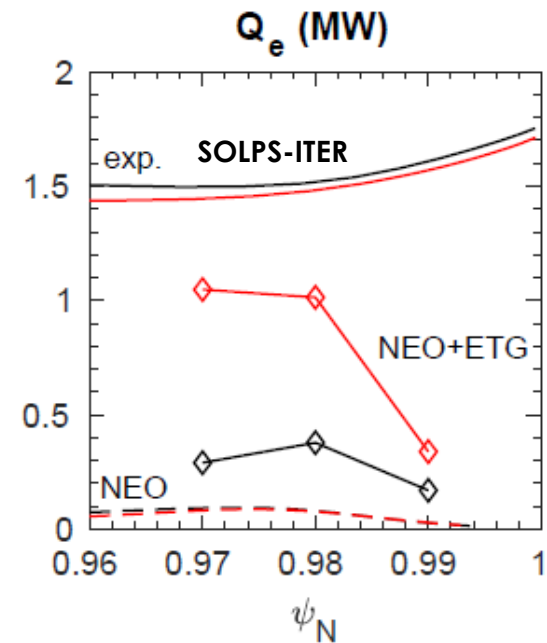
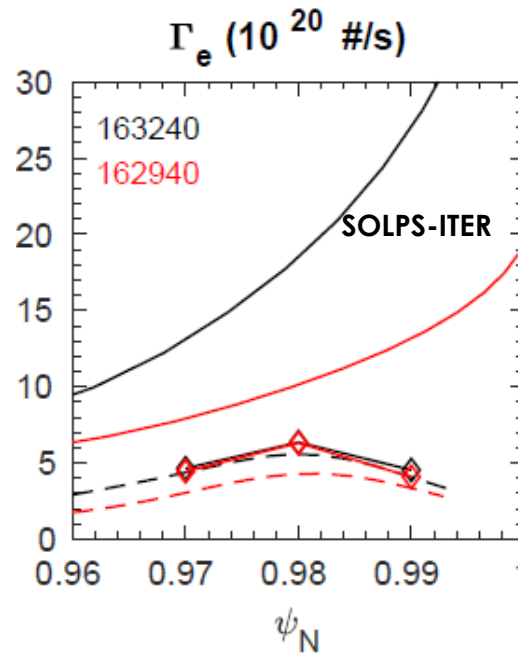
$Q_{e+i,TRANSP} = 2.8$ MW

- $Q_{ETG} + Q_{NEO}$ accounts for 30-60% of experimental Q_{e+i} (using scaled $\nabla n_e, \nabla T_e$)



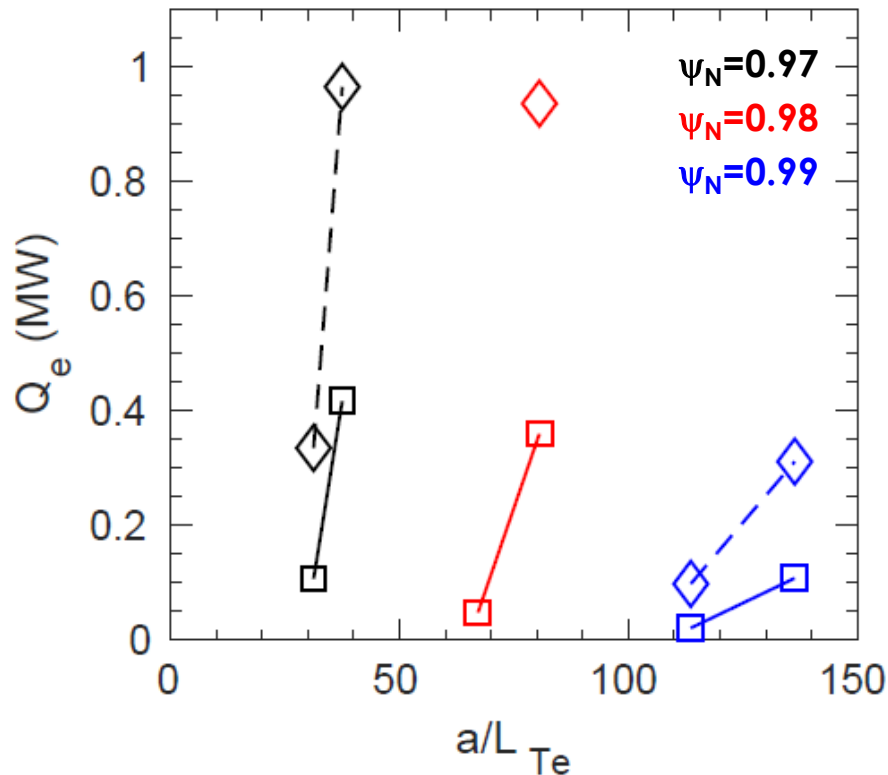
ETG (scaled gradients) + NEO recovers some, not all, of electron particle and thermal transport inferred from SOLPS-ITER

- Γ_e and Q_e agreement closer for closed divertor case
- Neoclassical $\Gamma_e \gg$ ETG Γ_e
- ETG + NC does not appear to account for all Γ_e & Q_e
- $(D_e/\chi_e)_{\text{SOLPS}} \sim 0.05\text{-}0.1$



Let's invert the problem \rightarrow predict profiles for given target fluxes, but we need transport model...

Additional simulations run to identify key dependencies with a/L_{Te} and a/L_{ne}

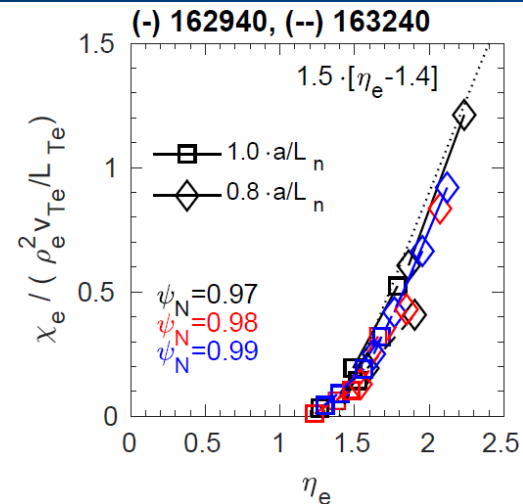


- Wide variation in predicted transport depending on density and temperature gradients

(solid) $1.0 \times a/L_{n,exp}$
(dash) $0.8 \times a/L_{n,exp}$

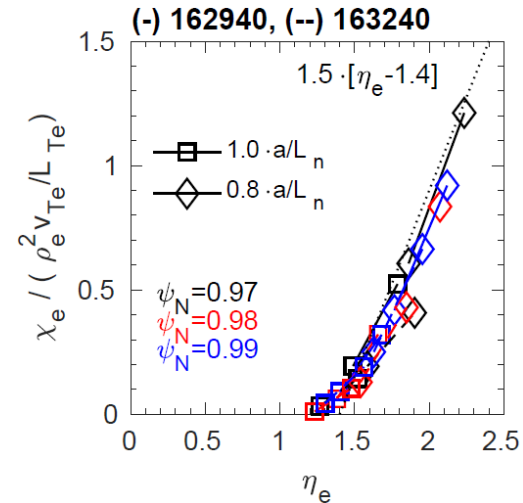
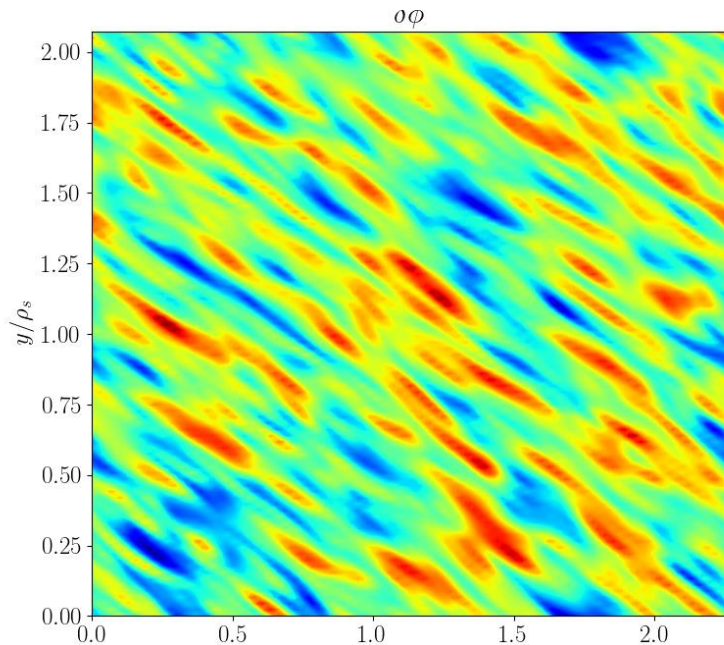
$\chi_{e,ETG}$ VS η_e overlap when using ETG-relevant electron gyroBohm (expected in “slab” limit, $L_{T,n}/R \ll 1$)

- $\sim O(1) \rho_e^2 v_{Te}/L_{Te}$ indicative of slab ETG transport, smaller than $\sim O(10)$ found for toroidal ETG [Jenko, Dorland 2000, 2002]



$\chi_{e,ETG}$ VS η_e overlap when using ETG-relevant electron gyroBohm (expected in “slab” limit, $L_{T,n}/R \ll 1$)

- $\sim O(1) \rho_e^2 v_{Te}/L_{Te}$ indicative of slab ETG transport, smaller than $\sim O(10)$ found for toroidal ETG [Jenko, Dorland 2000, 2002]

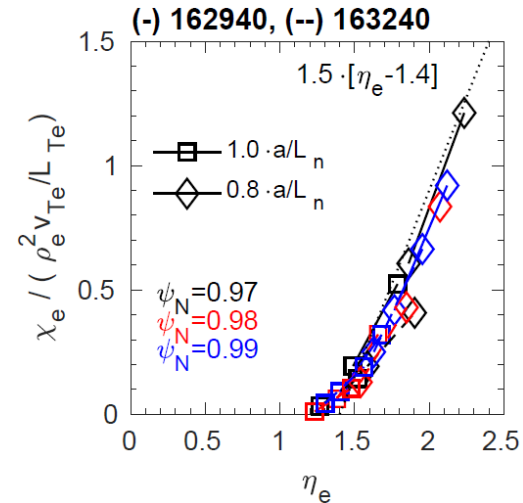


Eddies closer to isotropic than “streamers”
 ($L_x \sim 6 \rho_e < 15 \rho_e$ typical for core “streamers”)

Strongly tilted from large γ_E and s

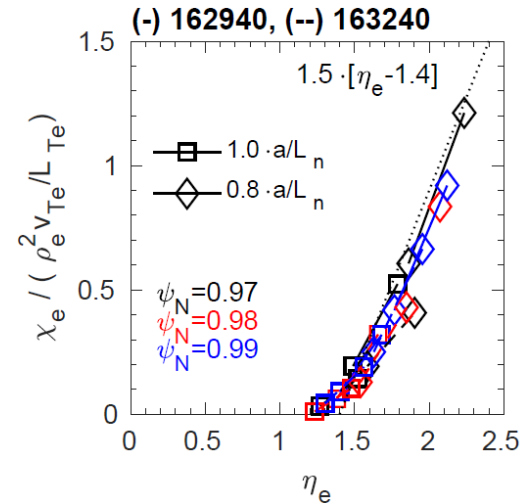
$\chi_{e,ETG}$ VS η_e overlap when using ETG-relevant electron gyroBohm (expected in “slab” limit, $L_{T,n}/R \ll 1$)

- $\sim O(1) \rho_e^2 v_{Te}/L_{Te}$ indicative of slab ETG transport, smaller than $\sim O(10)$ found for toroidal ETG [Jenko, Dorland 2000, 2002]
- Slab saturation explained by “Cowley secondary” instability [Cowley 1991] \rightarrow zonal flow driven by primary instability modes
 - Cowley secondary + high R/L \rightarrow large $k_{||}$, demands high parallel resolution ($n_\theta=[48,144,192]$ for $\psi_N=[0.97,0.98,0.99]$)



$\chi_{e,ETG}$ VS η_e overlap when using ETG-relevant electron gyroBohm (expected in “slab” limit, $L_{T,n}/R \ll 1$)

- $\sim O(1) \rho_e^2 v_{Te}/L_{Te}$ indicative of slab ETG transport, smaller than $\sim O(10)$ found for toroidal ETG [Jenko, Dorland 2000, 2002]
- Slab saturation explained by “Cowley secondary” instability [Cowley 1991] \rightarrow zonal flow driven by primary instability modes
 - Cowley secondary + high R/L \rightarrow large $k_{||}$, demands high parallel resolution ($n_\theta=[48,144,192]$ for $\psi_N=[0.97,0.98,0.99]$)
- Can infer a very simple reduced slab-ETG pedestal transport model



Regime of applicability:
 $R/L_{ne} \gg 1$

$$\chi_{e,ETG} = 1.5 \cdot [\eta_e - 1.4] \cdot \left(\frac{a/L_{Te}}{60} \right) \cdot \left(\frac{\rho_s^2 c_s}{a} \right)$$

Similar to GENE sims for AUG H-mode (Jenko, 2009)

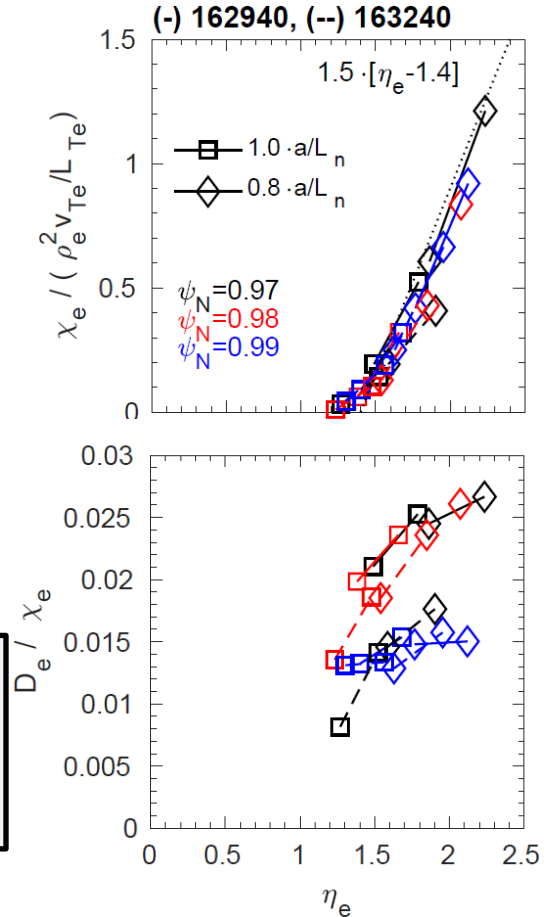
$\chi_{e,ETG}$ VS η_e overlap when using ETG-relevant electron gyroBohm (expected in “slab” limit, $L_{T,n}/R \ll 1$)

- $\sim O(1) \rho_e^2 v_{Te}/L_{Te}$ indicative of slab ETG transport, smaller than $\sim O(10)$ found for toroidal ETG [Jenko, Dorland 2000, 2002]
- Slab saturation explained by “Cowley secondary” instability [Cowley 1991] \rightarrow zonal flow driven by primary instability modes
 - Cowley secondary + high R/L \rightarrow large $k_{||}$, demands high parallel resolution ($n_\theta=[48,144,192]$ for $\psi_N=[0.97,0.98,0.99]$)
- Can infer a very simple reduced slab-ETG pedestal transport model

Regime of applicability:
 $R/L_{ne} \gg 1$

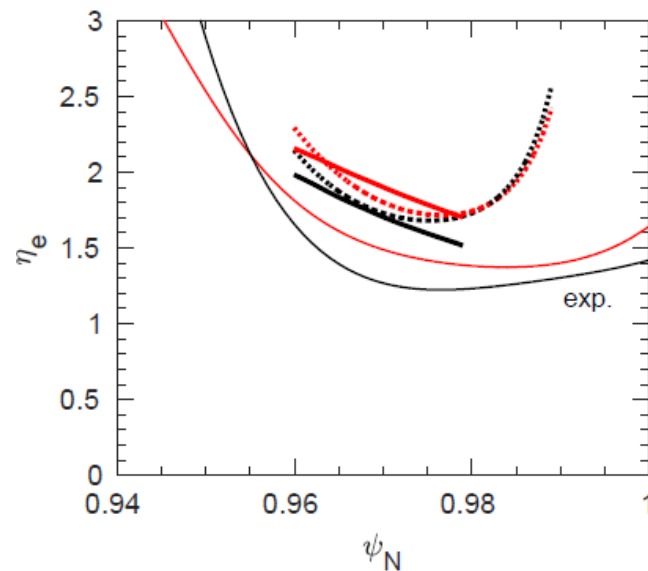
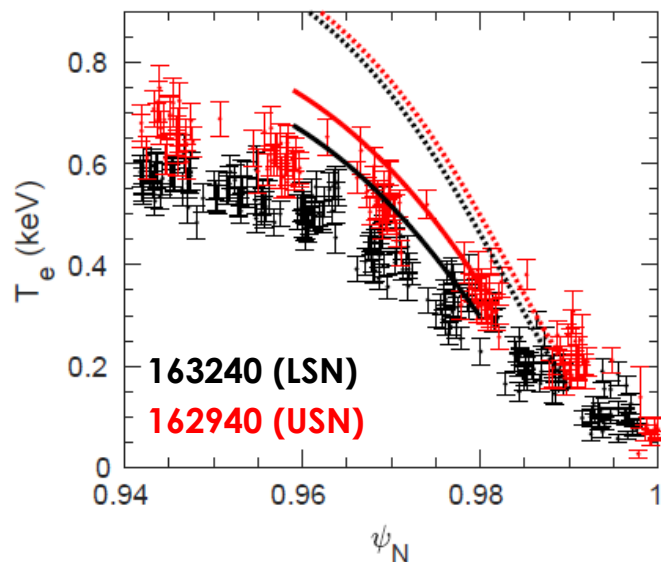
$$\chi_{e,ETG} = 1.5 \cdot [\eta_e - 1.4] \cdot \left(\frac{a/L_{Te}}{60} \right) \cdot \left(\frac{\rho_s^2 c_s}{a} \right)$$

$$D_{e,ETG} = 0.02 \cdot \chi_{e,ETG}$$



ETG transport model slightly over-predicts T_e (for fixed n_e); captures increase in T_e with lower n_e

- Captures increase in T_e and η_e with lower n_e (but mostly because $T_{e,BC}$ larger)
- Slight over-prediction of T_e ; gets worse if we move boundary out to $\psi_{N,BC}=0.99$
 - Difficult to overcome falling gyrobohm coefficient $Q_{GB} \sim T_e^{5/2}$

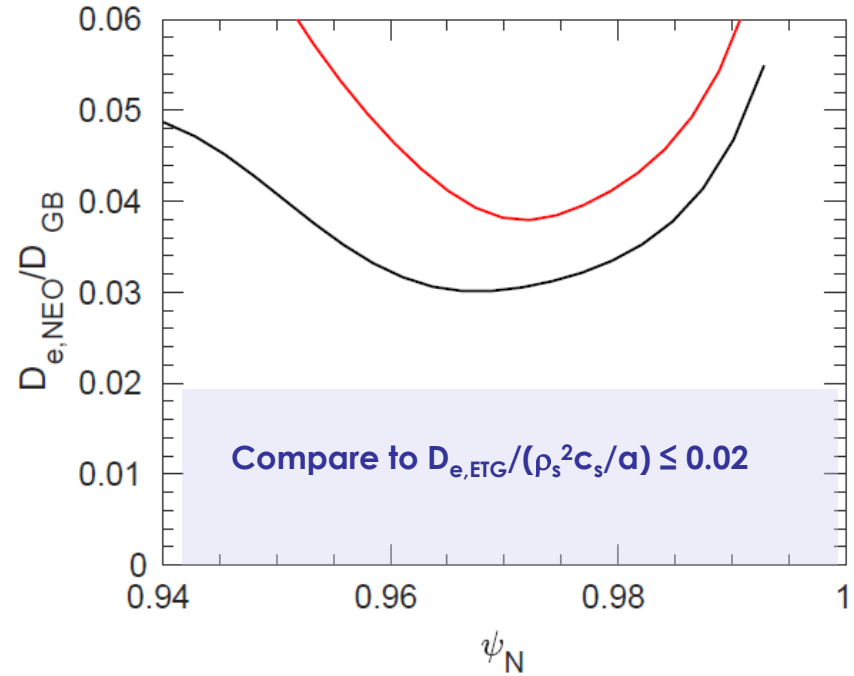


- Want to predict n_e & T_e simultaneously to see if sensitivities of transport with gradients improves / degrades agreement

To predict n_e , need to include neoclassical particle transport (larger than ETG contribution)

In the following $n_e + T_e$ predictions, we use:

- SOLPS-ITER Γ_e & Q_e for target fluxes
- Assumed constant $D_{e,NC} = 0.05 \cdot D_{GB}$



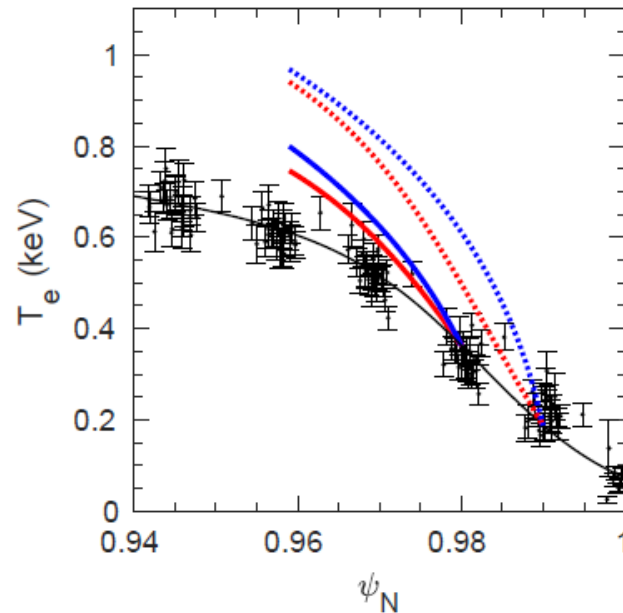
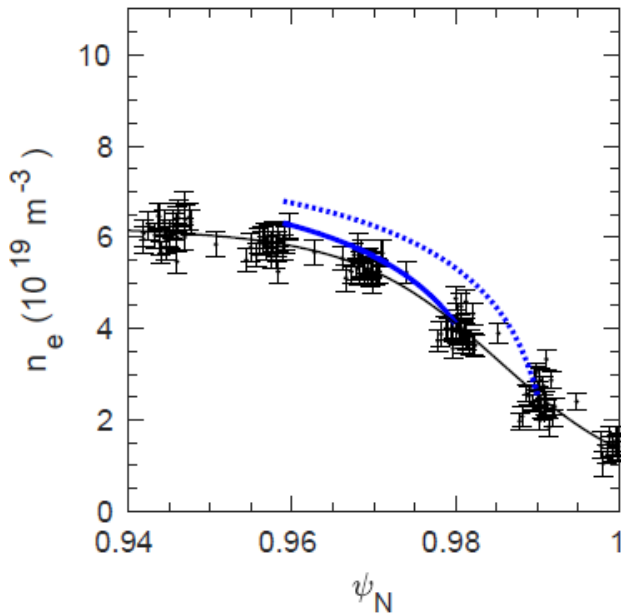
n_e & T_e predictions for closed divertor discharge similar to T_e only prediction

- $n_{e,\text{pred}} \sim n_{e,\text{exp}}$ (dominated by neoclassical Γ_e)
- Similar T_e over-prediction, gets worse as BC moved outward

162940 (closed divertor)

(red) T_e only prediction

(blue) n_e & T_e prediction



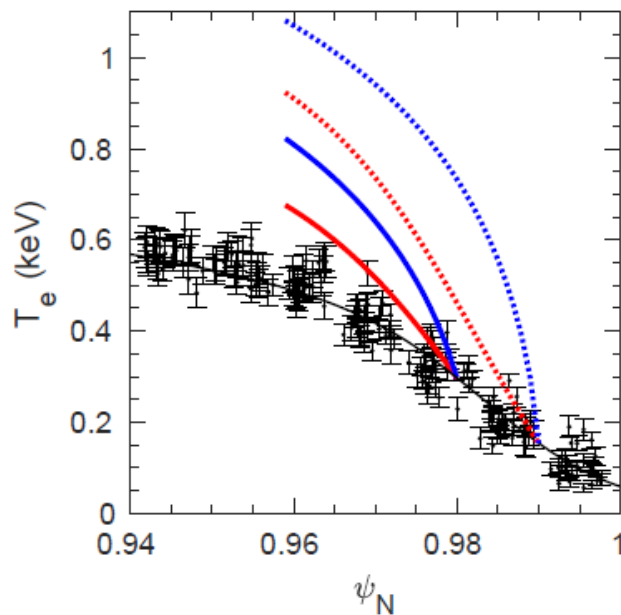
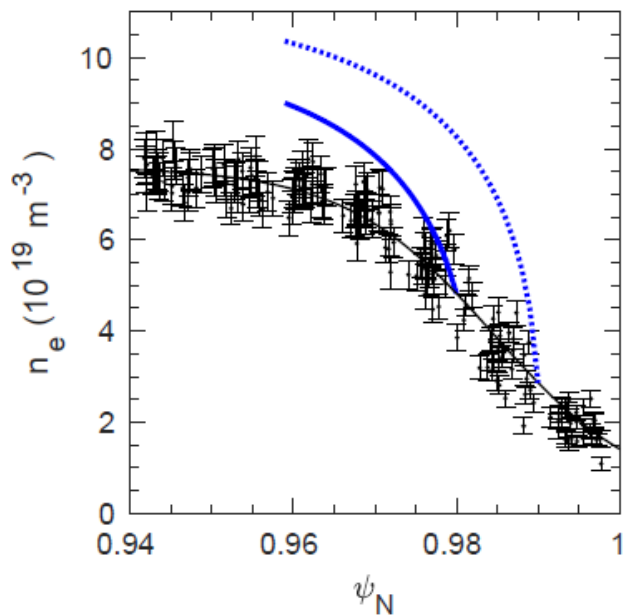
Much larger over-prediction for open divertor discharge (larger edge particle source)

- $\Gamma_{e,\text{open-divertor}} \sim \text{double the closed divertor case} \rightarrow \text{gives much larger } n_{e,\text{pred}} \text{ and corresponding } T_{e,\text{pred}}$

163240 (open divertor)

(red) T_e only prediction

(blue) n_e & T_e prediction



Much larger over-prediction for open divertor discharge (larger edge particle source)

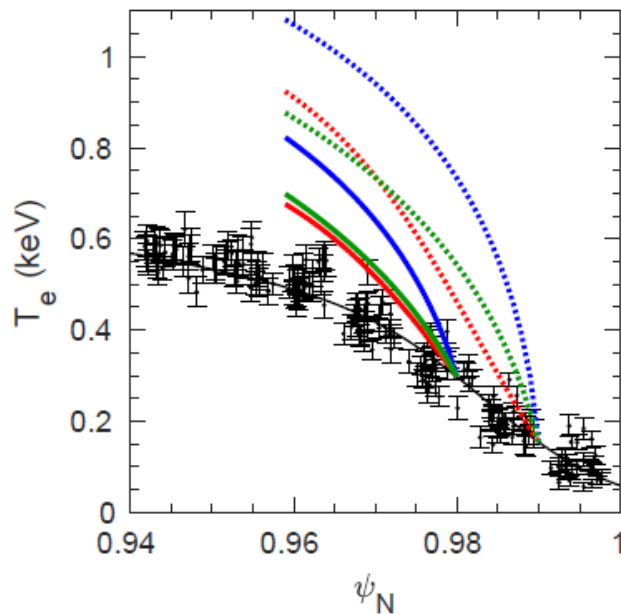
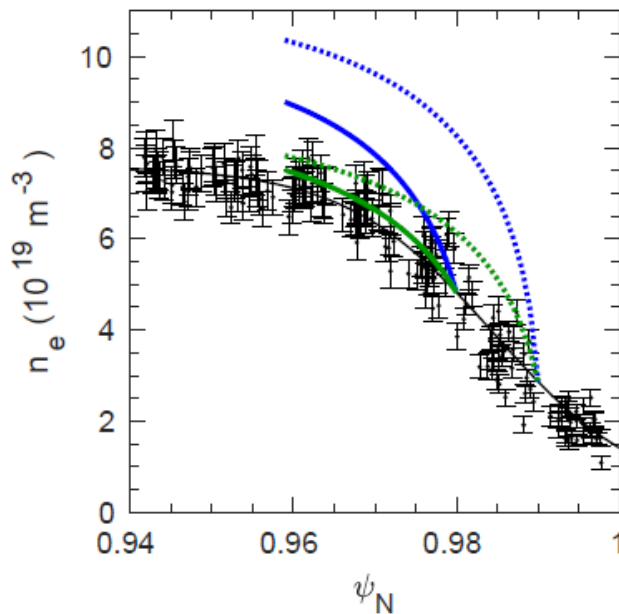
- $\Gamma_{e,open-divertor} \sim$ double the closed divertor case \rightarrow gives much larger $n_{e,pred}$ and corresponding $T_{e,pred}$
- Improved agreement if we use $\Gamma_{e,closed-divertor}$

163240 (open divertor)

(red) T_e only prediction

(blue) n_e & T_e prediction

(green) n_e & T_e prediction ($\Gamma_e = \Gamma_{e,closed divertor}$)



Plenty of uncertainties to investigate

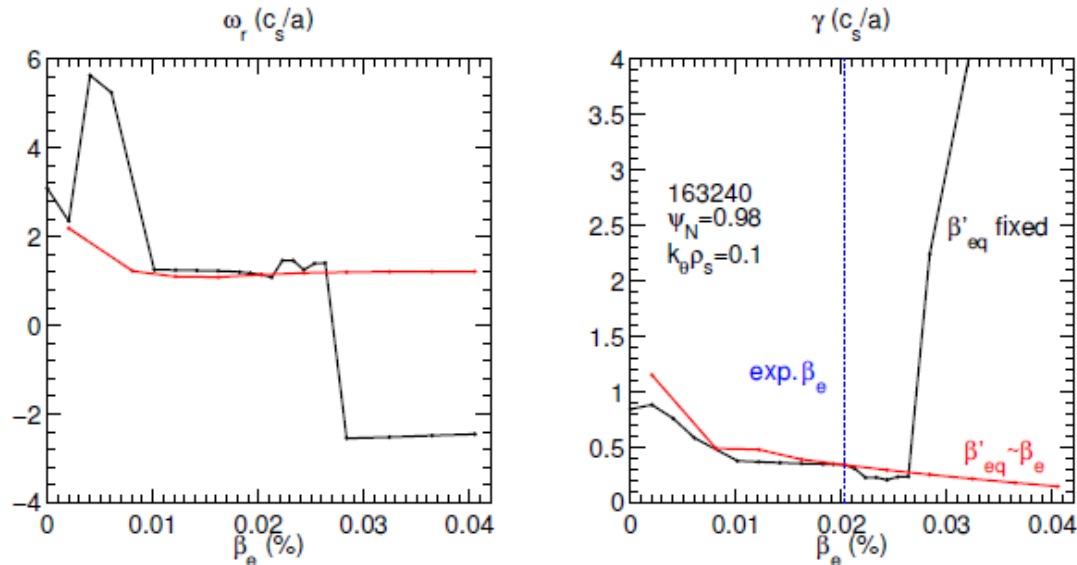
- **Sensitivity to T_i (e.g $T_d < T_c$ as in some main ion CX measurements [Haskey, 2018])**
 - Slab ETG not very sensitive: reducing $T_i/T_e=[1.47,2.45] \rightarrow 1$ for $\psi_N=[0.98,0.99]$ reduces $Q_{e,ETG} \sim 20\%$
 - Lower $T_{i,sep}$ / larger $\nabla T_{i,ped}$ increases neoclassical ion heat flux ($Q_{i,NEO}$ doubles for $T_d=T_e$)
 - Expect some impact on collisional coupling (Q_e / Q_i partition)
- **SOLPS-ITER analysis needs further validation and sensitivity tests to boundary conditions (may change inferred sources / fluxes)**
- **Need to self-consistently evaluate NEO and collisional exchange in the profile predictions**
 - ETG-model has been added to TGYRO, will test soon
- **More careful accounting for inter-ELM time-dependence in analysis and modeling**

Summary

- **Linear gyrokinetic analysis (CGYRO) suggests electron scale ETG turbulent transport may limit $\eta_e \sim \nabla T_e / \nabla n_e$ in some DIII-D ELMy H-mode pedestals**
- **Numerous *nonlinear* gyrokinetic simulations run to predict ETG transport, used to develop ETG pedestal transport model**
 - This is one of a few necessary pieces of a pedestal transport model
- **ETG contributes to $\chi_{e,ped}$, *but unlikely to be the only transport mechanism***
 - Ion-scale turbulence may contribute (simulations in progress)
 - Evidence for QCFs, recently interpreted as MTM [Diallo 2015, X. Liu, 2018 thesis]
 - Recent analysis suggests ion-scale turbulence becomes increasingly important for increasing pedestal widths $w/p_i > 10$ [Kotschenreuther, 2017]) → Similar result found in wide-pedestal grassy-ELM regime analysis [A. Ashourvan]
- **Neoclassical D_e plays non-negligible role in setting density profile**
 - Any additional transport mechanism must likely satisfy $D_e / \chi_e \ll 1$ for these shots (e.g. MTM)

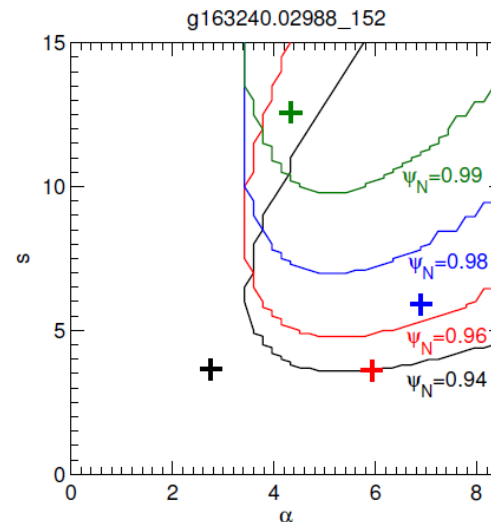
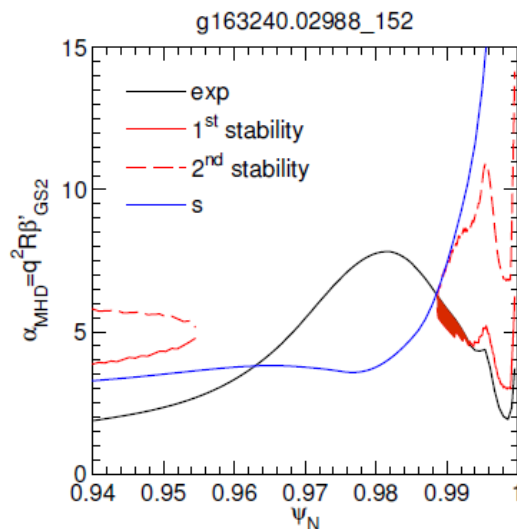
Electromagnetic effects stabilizing at $\psi_N=0.98$

- EM effects are stabilizing to ion scales modes in sharp gradient region
- β_e scans show $\psi_N=0.97-0.98$ is 15-20% below KBM threshold
 - 2nd stable if one varies $\beta'_{eq} \sim \beta_e$
 - Consistent with ideal infinite-n MHD ballooning simulations (next slide)



Small region in lower half of pedestal is sitting near ideal MHD infinite-n ballooning threshold

- Ideal MHD calculations (via 'ball') indicate lower half of pedestal near infinite-n ballooning stability boundary
 - Only $\Delta\psi=0.005$ surpasses threshold (out of $\Delta\psi_{\text{ped}}\sim 0.03$)
 - Region of sharpest gradient ($\psi_N=0.98$) is 2nd stable

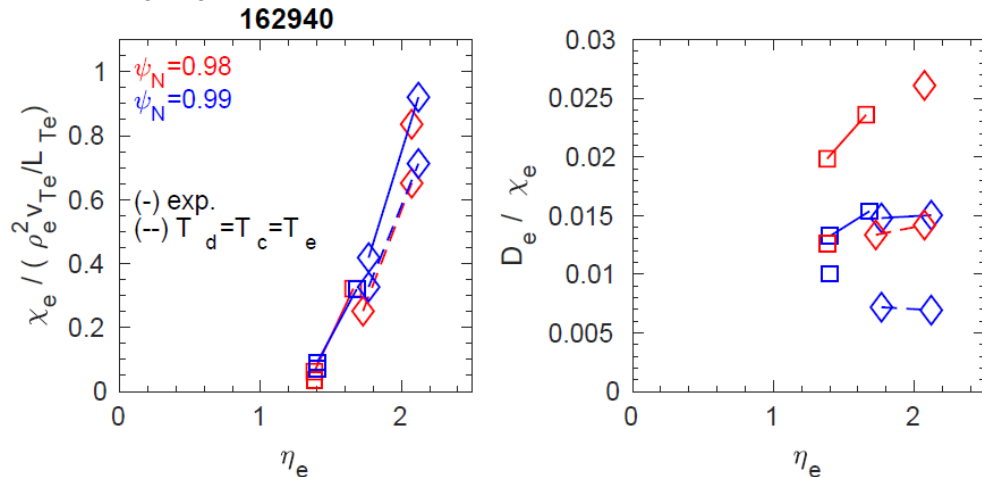


- Finite-n effects can remove 2nd stability [Snyder ...]

Testing $T_d=T_c=T_e$ in CGYRO NL ETG simulations (162940)

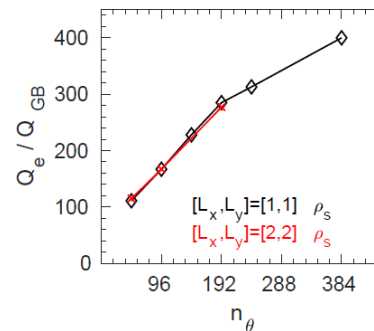
- Don't expect T_e/T_i to strongly influence slab ETG (need to revisit old theory papers)

- Reducing $T_i/T_e=[1.47,2.45] \rightarrow 1$ for $\psi_N=[0.98,0.99]$ reduces $Q_{e,ETG} \sim 20\%$
- Also lowers $D_e/\chi_e \sim 50\%$



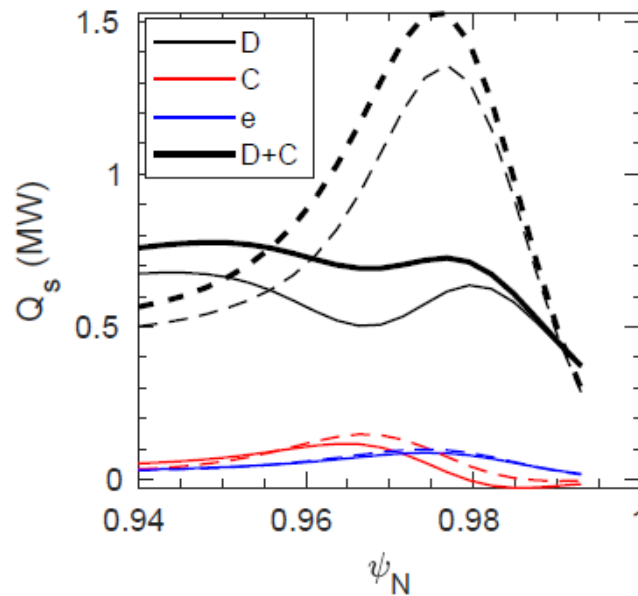
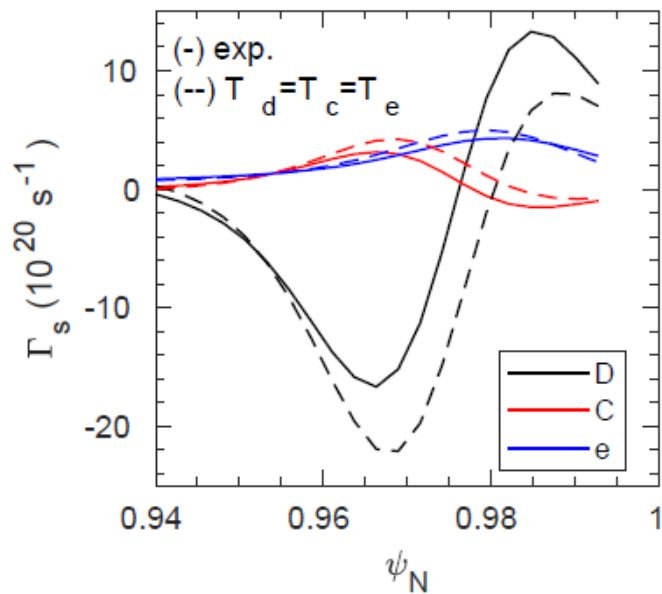
- Have also continued with resolution tests – going to $n_\theta=384$ ($\psi_N=0.99$) gives additional 30% increase \rightarrow

- $\sim 30\%$ uncertainty in leading coefficient of transport model



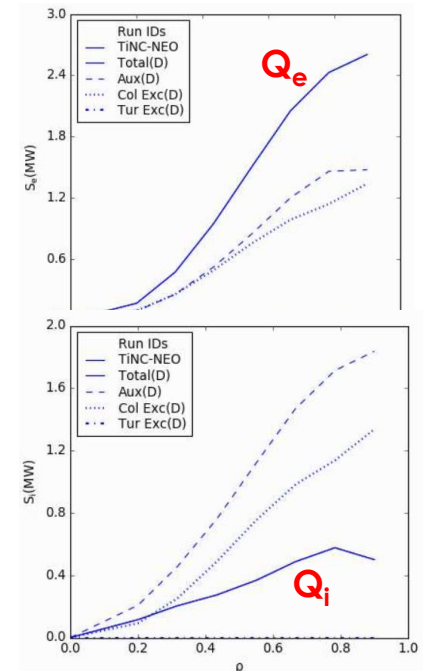
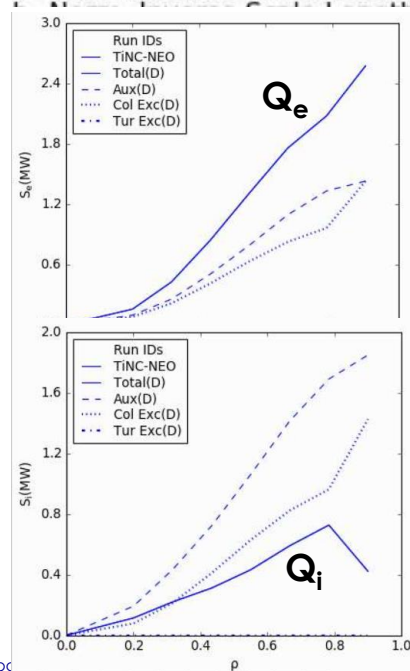
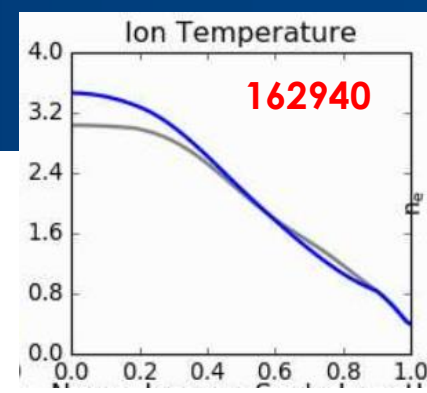
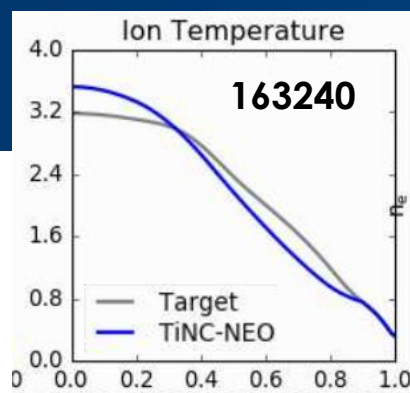
Testing $T_d=T_c=T_e$ in NEO simulations (162940)

- $Q_{i,NC} \sim$ doubles (0.5-0.7 MW \rightarrow 1-1.5 MW)



NC alone accounts for core Q_i

- Predictions of T_i -only using NEO+TGYRO (within OMFIT)
- Using fixed T_e , n_e , geometry ...
- Only $\chi_{i,NEO}$ (with dynamic energy exchange) gives $Q_{e,0.9} \sim 2.5$ MW
 - Larger than the ~ 1.5 MW used in above SOLPS-ITER analysis
- Perhaps this is an underpowered discharge (3 MW /)



Using simple transport solver to predict profiles

- Fixed equilibrium, T_i (and n_e , in this example)
- Use Q_e from SOLPS-ITER as target flux
- Set $T_{e,BC}$ to match experimental T_e fit at $\psi_N=0.98$ (or 0.99)
- Evaluate:

$$Q_{e,target} = Q_{e,model}(T_e, \nabla T_e; n_e, \langle \nabla V \rangle, B_{unit}, a)$$

at cell center ($i + \frac{1}{2}$) to solve for T_e^{i+1} , e.g.

$$T_{e,mid} = \frac{(T_e^{i+1} + T_e^i)}{2}$$

$$a \nabla T_e = \frac{(T_e^{i+1} - T_e^i)}{d(\frac{r}{a})}$$

- Not updating $i \rightarrow e$ collisional energy exchange

